J Mater Sci (2007) 42:9927–9933
DOI 10.1007/s10853-007-2078-8

Reaction synthesis of $TiC–TiB_2$/Al composites from an Al–Ti–B_4C system

Binglin Zou · Ping Shen · Qichuan Jiang

Received: 11 March 2007 / Accepted: 31 July 2007 / Published online: 9 September 2007

Abstract The $TiC–TiB_2$/Al composites were fabricated by self-propagating high-temperature synthesis (SHS) from Al–Ti–B_4C compacts. The addition of Al to the Ti–B_4C reactants facilitates the ignition occurrence, lowers the reaction exothermicity, and modifies the resultant microstructure. The maximum combustion temperature and combustion wave velocity decrease with the increase in the Al amount. The B_4C particle size exerts a significant effect on the combustion wave velocity and the extent of the reaction, while that of Ti has only a limited influence. The reaction products are primarily dependent on the B_4C particle size and the Al content in the reactants. Desired products consisting of only the TiC, TiB_2, and Al phases could be obtained by a cooperative control of the B_4C particle size and the Al content.

Introduction

Titanium carbide (TiC) and titanium diboride (TiB_2) ceramics possess desired properties such as low densities, high melting points, good thermal and chemical stability, high hardness and excellent wear resistance. In particular, use of these ceramics in composites offers the advantage of enhanced fracture toughness and wear resistance over the monolithic constituent, making them attractive for applications as advanced structural materials [1, 2].

B. Zou · P. Shen · Q. Jiang (✉)
Key Laboratory of Automobile Materials, Department of Materials Science and Engineering, Jilin University, No. 5988 Renmin Street, Changchun 130025, P.R. China
e-mail: jqc@jlu.edu.cn

Several techniques including reactive hot pressing [1, 3–5], transient plastic phase processing [6, 7], self-propagating high temperature synthesis (SHS) (also termed combustion synthesis) [2, 8–10], and spark plasma sintering [11] have been utilized to prepare the $TiC–TiB_2$ composites using Ti–B–C [2, 10], Ti–B_4C [1, 3–9], and Ti–B_4C–C [8, 9, 11] systems with proper proportions of the reactants. The reaction in these systems, however, is somewhat difficult to initiate because of the high melting temperatures of the reactants and lack of a preactivation reaction. Once initiated, however, it is explosive. The final products, on the other hand, are usually poorly consolidated and contain many cracks even though a dynamic compaction was employed immediately after the reaction was completed [8]. A possible solution to these problems is to incorporate the metals with low melting points and/or reasonable reactivity with titanium for formation of low-melting intermetallics into the reactants, as did in the Al–Ti–C [12, 13] and Ni–Ti–BN systems [14], where the addition of Al to Ti–C reactants was reported to significantly lower the reaction activation energy and decrease the exothermic extent [12, 13], and a small addition (1–3 wt.%) of Ni to Ti–BN reactants was found to substantially decrease the consolidation energy and time, promote the densification and improve the fracture toughness of the synthesized composites [14]. Such studies, however, were few in the Me(metal)–Ti–B_4C systems [3, 15]. For instance, with respect to the reaction in the Al–Ti–B_4C system, the first and simple investigation was performed by Gotman et al. [16], who fabricated the TiC and TiB_2 reinforced Al matrix composite with appreciable $TiAl_3$ phase via the SHS reaction from a 57.6 wt.% Al–Ti–B_4C preform with Ti:B_4C = 3:1 (in molar ratio). The maximum combustion temperature was reported to be 1,428 K and the combustion velocity to be 0.8 mm s^{-1}.

Another indirectly relevant study was from Taheri-Nassaj et al. [17], who obtained the final products of the Al–TiB_2–TiC composites, without the detectable $TiAl_3$ phase, by reactive spontaneous infiltration of molten Al into Ti–B_4C powder mixtures at 1,473 K. In addition, they suggested the following reactions:

$$3Al + Ti \rightarrow TiAl_3 \quad (1)$$

$$3TiAl_3 + B_4C \rightarrow 2TiB_2 + TiC + 9Al \quad (2)$$

More details on the reaction behavior and mechanism, however, were not presented. The lack of understanding of the reaction behavior and mechanism will certainly hinder the optimization of the processing, the resultant phases and their microstructure, and eventually the properties of the composites.

In a previous article [18], we have investigated the reaction mechanism in the self-propagating reactions of the Al–Ti–B_4C compacts, and in this article, we present the reaction behaviors and the resultant products. It is expected that the understanding of the reaction behaviors and mechanism would not only permit a better control of the reaction process through the regulation of processing variables, but also provide a concrete basis for the formulation of theoretical models that could be used as a guide for producing the TiC–TiB_2/Al composites with tailored microstructures and properties.

Experimental procedure

The raw materials used were commercial powders of Al (99 wt.% purity, ≤29 μm particle size), Ti (99 wt.%), and B_4C (~95 wt.%). The impurities in the B_4C powders were mainly free boron and carbon together with <1 wt.% Fe_2O_3. To examine the effect of the particle size, the B_4C particles with sizes of mainly ≤3.5 μm and within 3.5–50 μm (hereafter abbreviated as ≤50 μm) and the Ti particles varying from –500 mesh (≤28 μm) to –100 mesh (74–165 μm) were used [in most runs, however, the Ti particles of –300 mesh (37–48 μm) were used, except for those specifically indicated cases]. The proportion of Ti to B_4C was fixed to 3:1 in molar ratio and the Al content varied from 10 wt.% to 60 wt.% of the total weight of the mixtures. The reactant powders were mixed in a stainless-steel container for 8 h to ensure homogeneity. After mixing, the powders with suitable weights were uniaxially pressed into cylindrical compacts of ~22 mm in diameter and ~15 mm in height with green densities of ~65 ± 2% of theoretical, as determined from weight and geometric measurements. For comparison, limited numbers of the Ti–B_4C compacts were also prepared with the same dimensions and density.

The SHS experiments were conducted in a self-made vacuum vessel. The compact was placed on a graphite plate with a thickness of ~2.5 mm, below which a tungsten electrode was set up as the reaction ignition source. The vessel was first evacuated and then filled with Ar at 1 atm. The reaction was initiated by an arc heating, which was generated by passing a strong current between the tungsten electrode and the graphite plate. As soon as the reaction was initiated, the power was switched off. The temperature in close vicinity to the center of the compacts was measured by W5-Re26 thermocouples and the signals were recorded and processed by a data acquisition system using an acquisition speed of 50 ms/point. The combustion process was recorded by a CCD video camera using scanning speeds of 30–60 frames per second (depending on the reaction violent extent) to evaluate the combustion wave velocity. The phase compositions in the reacted samples were identified by X-ray diffraction (XRD, Rigaku D/Max 2500PC, Japan) and their morphology at the fracture surfaces was examined by scanning electron microscopy (SEM, JSM 5310, Japan) and field emission SEM (FESEM, JSM 6700F, Japan).

Results and discussion

Theoretical calculation of adiabatic temperature

The adiabatic temperature, T_{ad}, defined as the final theoretical temperature attained by a system undergoing an adiabatic condition, is a good measure of the exothermicity of the reaction and the state of the various phases. Providing (i) the self-propagating mode is initiated at room temperature (298 K) without any preheat, (ii) the reaction follows the overall equation of

$$xAl + 3Ti + B_4C \rightarrow 2TiB_2 + TiC + xAl \quad (3)$$

and (iii) no eutectic transformation (TiC + TiB_2 ⇔ Liquid [19]) occurs in the resultant TiC and TiB_2 phases, the value of T_{ad} for the reaction in the Al–Ti–B_4C system could be calculated using thermodynamic data from references [20, 21] according to the following equation [22],

$$\Delta H(298) + \int_{298}^{T_{ad}(298)} \sum n_j C_p(P_j) dT + \sum_{298-T_{ad}(298)} n_j L(P_j) = 0 \quad (4)$$

where $\Delta H(298)$ is the reaction enthalpy at 298 K, n_j is the stoichiometric numbers, C_p and L are the heat capacity and latent heat (including melting and boiling), and P_j refers to the product, respectively. The calculated T_{ad} values as a function of the reactant Al weight percent are shown in

Fig. 1 together with the experimentally determined maximum combustion temperatures (T_c), as will be described later. It may be mentioned that the phase and microstructural examinations on the synthesized samples with high Al contents revealed the presence of some intermediate phases such as $TiAl_3$ and Al_4C_3, which were not considered here. According to Merzhanov's empirical criterion, for the reaction to be self-sustaining in the absence of preheat, T_{ad} should not be less than 1,800 K [23], implying a maximum addition of 52.2 wt.% Al in the reactants.

Reaction behavior and phase identification

The variation in the maximum combustion temperature, T_c, with the Al weight percent (w_{Al}) in the case of using two sizes of the B_4C particles is shown in Fig. 1 for a better comparison with the value and the behavior of T_{ad}. With the increase in w_{Al}, both T_{ad} and T_c decrease substantially. The effect of the B_4C particle size on the combustion temperature, however, is insignificant except for $w_{Al} > 40\%$. It was experimentally observed that when $w_{Al} = 50\%$, the self-sustaining reaction was successful in the samples with ≤3.5 μm B_4C particles but failed in those with ≤50 μm B_4C particles unless a prolonged arc heating was supplied. For $w_{Al} \geq 60\%$, the reaction in all the samples could no longer be self-sustaining without a noticeable preheating effect, regardless of the B_4C particle size. Such a behavior is generally consistent with the aforementioned

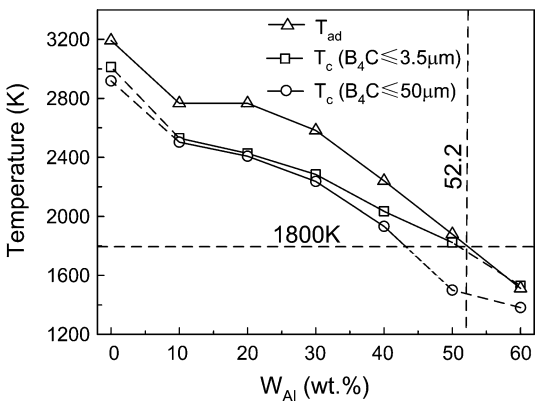

Fig. 1 Variations in the theoretically calculated adiabatic temperature, T_{ad}, and experimentally determined maximum combustion temperature, T_c, with the Al weight percent (w_{Al}) using two sizes of the B_4C particles. It is worthwhile to mention that the T_c values for the Ti–B_4C samples are far beyond 2,573 K and they were determined by extrapolation from the available temperature-electromotive force function, which might have a relatively large error. On the other hand, T_c for the samples with 60 wt.% Al and 50 wt.% Al with $B_4C \leq 50$ μm could be affected by the prolonged arc heating since the reaction was unable to self-sustain after removal of the heater. Therefore, the corresponding T_c values are connected by dashed lines in the figure

theoretical prediction of the maximum addition of 52.2 wt.% Al in the reactants for the reaction to be self-sustaining. The measured T_c values, on the other hand, are smaller than T_{ad} when $w_{Al} \leq 50\%$ because of heat loss. However, the difference between them seems to decrease with an increase in the amount of Al when the small B_4C particles were used. A prolonged heating for the ignition could bring a preheating effect in high Al content ($w_{Al} \geq 50\%$) samples and thus increases the combustion temperature. Besides, the decreasing maximum combustion temperature with the increasing Al content also reduces the heat loss in unit time, thus making the difference between T_c and T_{ad} smaller.

Figure 2 shows the variation in the ignition delay time (t_{ig}), which represents the time interval from the onset of heating to the initiation of the SHS reaction, with w_{Al} when the B_4C particle was 3.5 μm. As can be seen, t_{ig} first decreases and then increases with the increase of w_{Al}, indicating that the SHS reaction initiated more readily at a specific amount of Al (e.g., 30 wt.% Al in the present study). Previous examinations [18] on the reaction and phase formation mechanisms have demonstrated that the primary reaction between Ti and B_4C could be promoted by the addition of Al through the formation of low-melting $TiAl_n$ intermetallics (initially, the $TiAl_3$ phase), which provides a much better particle contact and thus reduces atomic diffusion distance and decreases the diffusion and reaction activation energies. However, with the further increase of w_{Al}, t_{ig} increases substantially because the heat liberated by the reaction decreases significantly, as reflected by T_{ad} and T_c in Fig. 1. Consequently, the value of t_{ig} shows first a decrease and then an increase behavior.

Figure 3 shows the dependence of the combustion wave velocity on the Al content as well as on the B_4C particle size. Clearly, the wave velocity decreases monotonically with the increase in the Al content. This result is somewhat different from that observed in the Al–Ti–C system, where

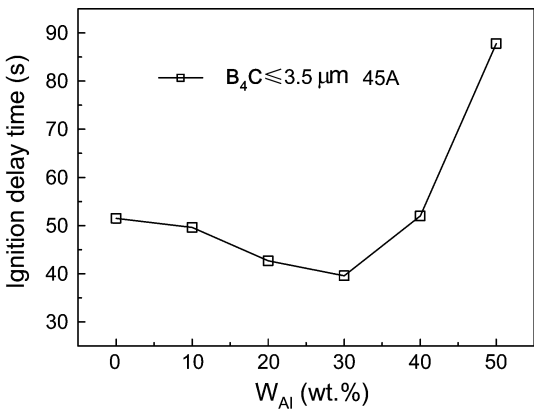

Fig. 2 Variation in the ignition delay time (t_{ig}) with the Al weight percent (w_{Al})

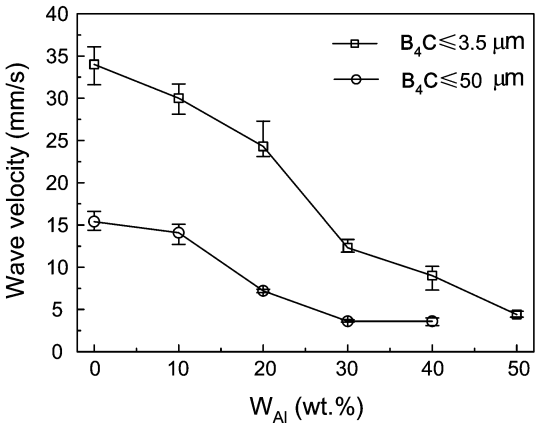

Fig. 3 Dependence of the combustion wave velocity on the Al content for two sizes of the B_4C particles used

the wave velocity displays a maximum value for the Al content in the range of 15–25 wt.% [12]. The B_4C particle size has a significant effect on the combustion wave velocity. The velocity decreases rapidly as the B_4C particle size changes from ≤3.5 μm to ≤50 μm, particularly when the Al content is low. This could be explained by the expression for the velocity of propagation based on a diffusion model [24]

$$V^2 = \frac{2K}{d^2 c_p \rho S} D_0 \exp(-E/RT_c) \quad (5)$$

where V is the wave velocity, c_p is the heat capacity of the product, ρ is the density of the product, d is the particle size of one of the reactants, S is the stoichiometric ratio of the reactants, D_0 is the diffusion preexponential coefficient, K is a constant, R is the gas constant, and E is the activation energy for the process. Assuming that the other parameters do not vary significantly with the B_4C particle size, an increase in the particle size could lead to a decrease in the wave velocity in an equivalent scale.

Figure 4 shows the XRD results of the reaction products for the samples with various Al contents and two different B_4C particles. As indicated, the reaction products depend not only on the Al content but also on the B_4C particle size. For $w_{Al} \leq 20\%$, the reaction products consist of TiB_2 and TiC binary phases in the reacted Ti–B_4C samples and TiB_2, TiC, and Al in the reacted Al–Ti–B_4C samples, without any intermediate phases, indicating that the reactions are complete even when the coarse B_4C particles (≤50 μm) were used. For w_{Al} = 30–40%, the reaction products are slightly different in the samples with different sizes of the B_4C particles. Only TiB_2, TiC, and Al are detected in the samples with ≤3.5 μm B_4C particles, but in those with ≤50 μm B_4C particles, in addition to the aforementioned primary phases, a small amount of $TiAl_3$ is also observed. With a further increase in w_{Al}, the reaction products are substantially different in these two kinds of the samples. For the samples with the fine B_4C (≤3.5 μm) particles, the reaction products consist of the primary Al, TiB_2, and TiC phases together with some $TiAl_3$ or/and Al_4C_3 intermediate phases; while for the samples with the coarse ones (≤50 μm), the primary phases are $TiAl_3$, Al, and unreacted B_4C, suggesting that the dominating reaction occurs between Al and Ti. These results, in turn, explain the dependence of the combustion temperature on the Al content and the B_4C particle size, as shown in Fig. 1.

Figure 5 shows the effects of the Ti particle size on the maximum combustion temperature and combustion wave velocity for the 40 wt.% Al–Ti–B_4C samples, and Fig. 6 gives the selected XRD results of the reaction products. Compared with that of B_4C, the effect of the Ti

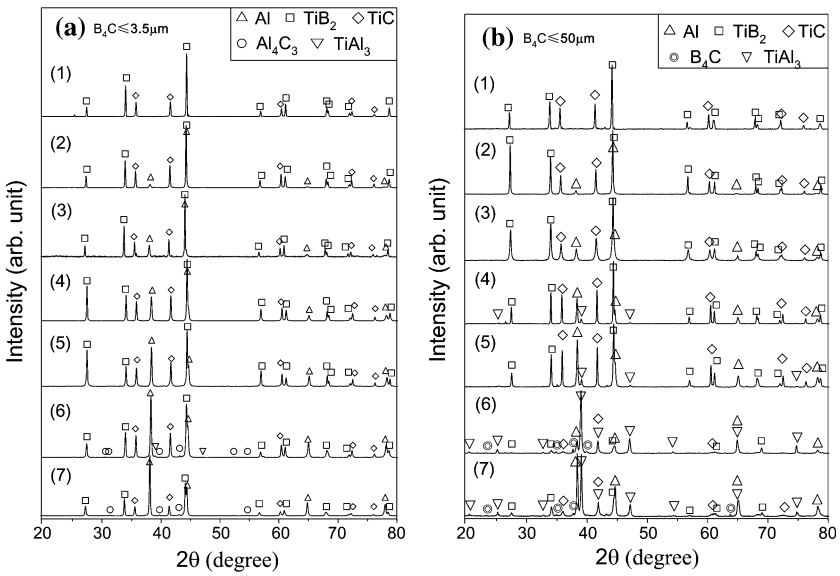

Fig. 4 XRD patterns of the SHS reaction products in the samples with various Al contents for two sizes of the B_4C particles [(**a**) $B_4C \leq 3.5$ μm and (**b**) $B_4C \leq 50$ μm] used: (1) 0 wt.% Al, (2) 10 wt.% Al, (3) 20 wt.% Al, (4) 30 wt.% Al, (5) 40 wt.% Al, (6) 50 wt.% Al, and (7) 60 wt.% Al

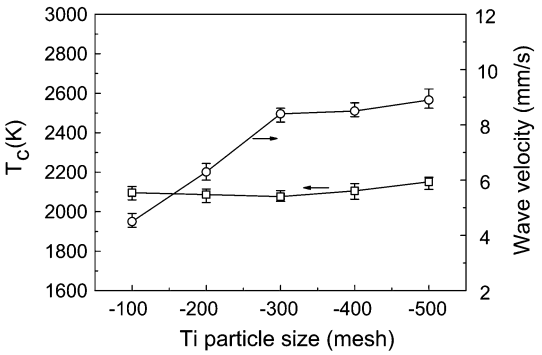

Fig. 5 Effects of the Ti particle size on the maximum combustion temperature and combustion wave velocity for the 40 wt.% Al–Ti–B_4C samples

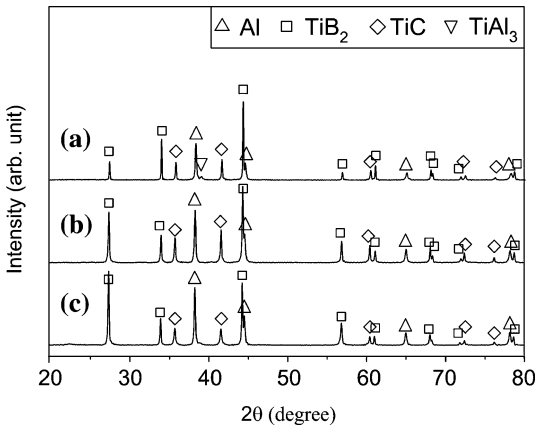

Fig. 6 XRD patterns of the SHS reaction products in the 40 wt.% Al–Ti–B_4C samples with the Ti particle sizes of (**a**) –100 mesh, (**b**) –300 mesh, and (**c**) –500 mesh

particle size is far less significant. With the decrease in the Ti particle size, the combustion temperature does not vary considerably and the wave velocity first exhibits an appreciable increase and then tends to be constant. The reaction products consist of the Al, TiB_2, and TiC phases except for the case of using the –100 mesh (74–165 μm) Ti particles, in which a small amount of $TiAl_3$ phase was found. This is not difficult to understand since most of the Ti particles react with Al to form titanium aluminides and the maximum combustion temperatures are generally higher than the melting points of both titanium aluminides and Ti. The titanium aluminides and the Ti particles (if not completely consumed) would melt during the passage of the combustion wave, making the role of the Ti particle size not so significant as that of B_4C. Likewise, the effect of the Al particle size, although not examined in the present study, is thought to be of little importance.

Microstructures

Figure 7 shows the typical agglomeration microstructures at the fracture surfaces of the reacted Ti–B_4C samples. For the small B_4C particles (≤3.5 μm) used, a fine hypereutectic-type structure was observed in the products (Fig. 7a), suggesting that a eutectic reaction involving the TiC and TiB_2 phases might progress during the synthesis process. For the large B_4C particles (≤50 μm) used, however, no such eutectic structure but a large amount of bulky TiB_2 clusters were observed (Fig. 7b). It was reported by Gusev [19] that the eutectic reactions could take place in the TiC_x–TiB_2 system. The eutectic composition and temperature are dependent on the stoichiometry (x) of TiC_x, e.g., when $x = 0.6$, the eutectic point is for 40.1 mol.% TiB_2 at 2,910 K, and when $x = 1.0$, the eutectic point is for 40.2 mol.% TiB_2 at 2,936 K. The experimentally determined maximum combustion temperatures in the samples with the small B_4C particles (≤3.5 μm) are about 2,965–3,045 K, slightly above the aforementioned eutectic temperatures. Therefore, the occurrence of the eutectic transformation is possible in

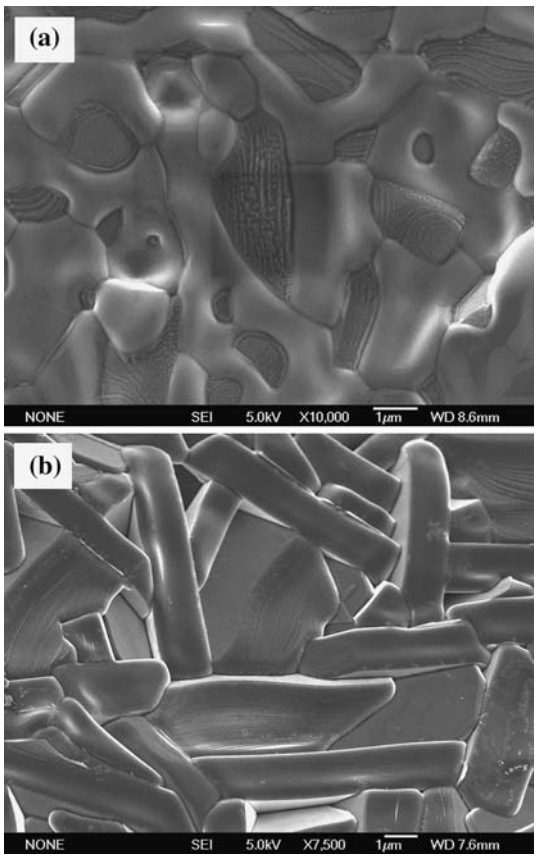

Fig. 7 FESEM micrographs showing the typical agglomeration microstructures at the fracture surfaces of the reacted Ti–B_4C samples for two sizes of the B_4C particles used: (**a**) ≤3.5 μm and (**b**) ≤50 μm

those samples and the microstructure in Fig. 7a consists of the primary TiB_2 phase and the encircled eutectic TiC_x–TiB_2 phases, i.e., a hypereutectic microstructure because of 66.7 mol.% TiB_2 in the products. On the other hand, the maximum combustion temperatures in the samples with the large B_4C particles are about 2,883–2,948 K, just close to or even lower than the eutectic temperatures. Hence, the eutectic structure was unable to develop or was only weakly developed.

Figure 8 shows the typical microstructures at the fracture surfaces of the reacted Al–Ti–B_4C samples ($B_4C \leq 3.5$ μm) with various Al contents. As indicated, the microstructures in the Al–Ti–B_4C samples are quite different from those in the Ti–B_4C samples. The individual TiC and TiB_2 grains were largely developed, without forming a eutectic-like structure. TiC exhibits sphere or round shapes and TiB_2 presents hexagonal or rectangular shapes. With the increase in the Al amount, the quantity of the TiC and TiB_2 grains decreases and their size changes from several micrometers to several hundreds of nanometer. The reduction in size is mainly caused by the decrease in the maximum combustion temperature as a function of increasing w_{Al}. Moreover, in some regions, the TiC and TiB_2 grains are separately located (e.g., only the large and small TiC grains were found in Fig. 8b), which could be essentially attributed to the much higher dissociation and diffusion rates of carbon from the B_4C crystal into the Ti–Al melt than those of boron, as we have described thoroughly in a previous paper [18].

Conclusions

Based on the preceding results, the following conclusions could be drawn:

(1) Theoretical estimation of adiabatic temperatures shows that the reaction in the Al–Ti–B_4C system could be self-sustainable for the presence of no more than 52.2 wt.% Al in the reactants without any preheat, which is generally consistent with the experimental observation.

(2) The proper addition of Al to the Ti–B_4C reactants not only lowers the ignition delay time but also reduces the reaction exothermicity and modifies the resultant microstructures. Increasing the Al content in the reactants considerably decreases the maximum combustion temperature and combustion wave velocity.

(3) The B_4C particle size has a significant effect on the ignition behavior and combustion wave velocity while that of Ti has only a limited influence. Increasing the B_4C particle size retards the reaction initiation and remarkably lowers the combustion velocity. The maximum combustion temperature, however, is not significantly affected as long as the reaction could get to completion.

(4) The reaction products are dependent on the B_4C particle size and the Al content. Ideal phases consisting of only TiC, TiB_2, and Al could be obtained by a cooperative control of the B_4C particle size and the Al content.

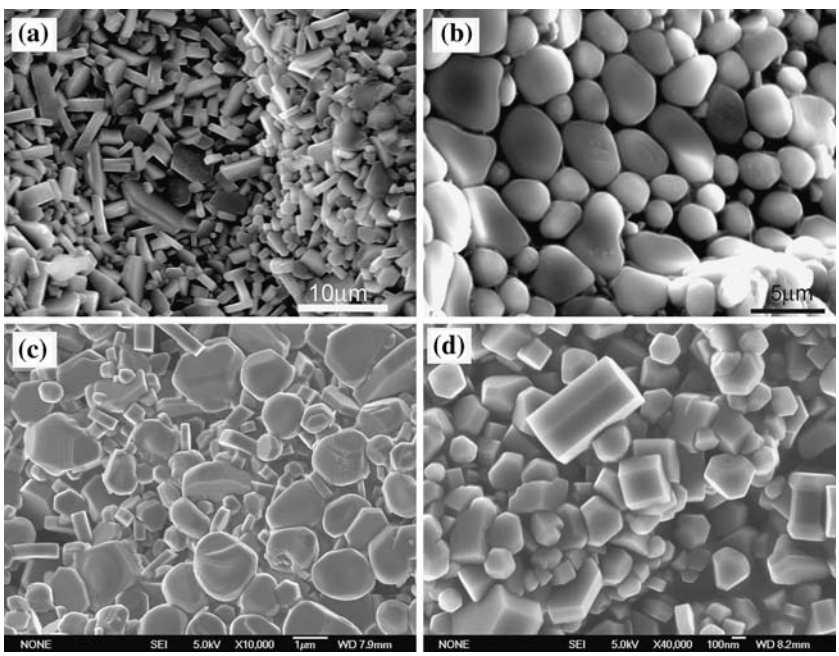

Fig. 8 SEM (**a**, **b**) and FESEM (**c**, **d**) micrographs showing the typical microstructures at the fracture surfaces of the reacted Al–Ti–B_4C samples ($B_4C \leq 3.5$ μm) with various Al contents: (**a**) 10 wt.% Al, (**b**) 20 wt.% Al, (**c**) 40 wt.% Al, and (**d**) 60 wt.% Al

Acknowledgement This work is supported by The National Natural Science Foundation of China (Project No. 50531030) and the Ministry of Science and Technology of China (No. 2005CCA00300) as well as by the Project 985-Automotive Engineering of Jilin University.

References

1. Wen G, Li SB, Zhang BS, Guo ZX (2001) Acta Mater 49:1463
2. Bhaumik SK, Divakar C, Singh AK, Upadhyaya GS (2000) Mater Sci Eng A279:275
3. Gotman I, Travitzky NA, Gutmanas EY (1998) Mater Sci Eng A244:127
4. Li SB, Zhang BS, Wen GW, Xie JX (2003) Mater Lett 57:1445
5. Zhao H, Cheng YB (1999) Ceram Inter 25:353
6. Barsoum MW, Houng B (1993) J Am Ceram Soc 76:1445
7. Brodkin D, Kalidindi SR, Barsoum MW, Zavaliangos A (1996) J Am Ceram Soc 79:1945
8. Song I, Wang L, Wixom M, Thompson LT (2000) J Mater Sci 35:2611
9. Zhang XH, Zhu CC, Qu W, He XD, Kvanin VL (2002) Compos Sci Technol 62:2037
10. Contreras L, Turrillas X, Vaughan GBM, Kvick Å, Rodríguez MA (2004) Acta Mater 52:4783
11. Locci AM, Orrù R, Cao G, Munir ZA (2006) J Am Ceram Soc 89:848
12. Choi Y, Rhee SW (1993) J Mater Sci 28:6669
13. Lee WC, Chung SL (1997) J Am Ceram Soc 80:53
14. Rangaraj L, Divakar C (2004) J Am Ceram Soc 87:1872
15. Lee SK, Kim DH, Kim CH (1994) J Mater Sci 29:4125
16. Gotman I, Koczak MJ, Shtessel E (1994) Mater Sci Eng A187:189
17. Taheri-Nassaj E, Kobashi M, Choh T (1997) Scripta Mater 37:605
18. Shen P, Zou BL, Jin SB, Jiang QC (2007) Mater Sci Eng A 454–455:300
19. Gusev AI (1997) J Solid State Chem 133:205
20. Liang YJ, Che YC (1993) Handbook of thermodynamic data of inorganics. Northeastern University Press, ShenYang (in Chinese)
21. Barin I (1995) Thermochemical data of pure substances, 3rd edn. Wiley-VCH Verlag GmbH, Germany
22. Moore JJ, Feng HJ (1995) Prog Mater Sci 39:243
23. Novikov NP, Borovinskaya IP, Merzhanov AG (1975) In: Merzhanov AG (ed) Combustion processes in chemical technology and metallurgy. Chernogolovka, p 174
24. Hardt AP, Phung PV (1973) Combust Flame 21:77